Gas-Phase Reactivity of $(C_5H_5Mg)^+$ Complexes: An Experimental and Theoretical Study

J. Berthelot, A. Luna, and J. Tortajada*

Laboratoire de Chimie Organique Structurale, Université Pierre et Marie Curie, CNRS UMR 172, Boîte 45, 4 Place Jussieu, F-75252 Paris Cedex 05, France

Received: March 19, 1998; In Final Form: May 11, 1998

The gas-phase reactivity of $C_5H_5Mg^+$ complexes generated from ionized magnesocene $(Cp)_2Mg^{\bullet+}$ have been investigated by means of tandem mass spectrometry. Decomposition of metastable $C_5H_5Mg^+$ ions involves the metal−ligand dissociation and a hydrogen atom elimination leading to the formation of Mg^+ and C_5H_4-$Mg^{\bullet+}$ ions. Collisional activation induces further fragmentations, yielding $C_3H_3Mg^+$ and $C_3H_2Mg^{\bullet+}$ ions. To have some insight into the structure and energetics of these four series of complexes, high-level ab initio calculations (G2(MP2)) have been performed. In addition, the nature of the metal ion−ligand interaction, the charge distribution, as well as the characterization of orbitals involved in relevant systems have been analyzed by using the atoms in molecules theory (AIM) of Bader and the natural bond orbital (NBO) analysis. The $Cp^{\bullet}\cdots Mg^+$ binding energy has been estimated to be 74.0 kcal/mol, over the cyclopentadienyl geometry optimized at the CASSCF level both for $^2B_1$ and $^2A_2$ electronic states.

Introduction

Over the past years, the study of gas-phase organometallic ion chemistry has experienced a rapid growth. This increased activity has been stimulated by the need for physical data on organometallic species and a better understanding of the reactivity of metallic or organometallic ions with a variety of inorganic or organic compounds.[1]

In this respect a wide variety of mass spectrometric techniques[2] has been used in these studies, giving a large amount of thermochemical, kinetic, and mechanistic information that has been used to evaluate the energetics of catalytic processes and the feasibility of proposed reaction pathways.

These experimental investigations are more and more complemented by theoretical calculations that provide not only the structures and binding energies for the given metal−ion complexes but also a description of the associated potential energy surfaces. These studies are particularly scarce for transition metal−ion complexes. The difficulties in a quantitative theoretical description of the bonding in compounds involving transition metals arise from the presence of quasi-degenerated d electrons that necessitates very high-level ab initio calculations in order to get accuracy, as shown by Pierloot et al.[3]

Among neutral organometallic species having no d electrons, organomagnesium compounds have received considerable attention because of their importance in organic synthesis. The magnesocene is one of the most well-known. Prepared for the first time in 1954 by Wilkinson and Cotton,[4] its structural features are well established[5] and the "π-sandwich" structure has been corroborated by ab initio calculations.[6] Magnesocene ($MgCp_2$) is of particular interest because it has found several applications as a host molecule for EPR investigations[7] and as a precursor for photolytic deposition of magnesium in the growing electronics/semiconductors industry.[8,9]

Even if some studies have also been devoted to the structure and bonding patterns of radical MgCp,[10] as well as some other metallic homologue systems M−Cp for several metals[11] M, little work has been done on the corresponding cation species $MgCp^+$. Recently,[12] some results for the reaction of the ground state of $MgCp^+$ with a variety of H-, N-, O-containing ligands (N_2, NH_3, CO, ...) have been reported, but to the best of our knowledge, the structure, the bonding characteristics, and the unimolecular reactivity of $MgCp^+$ has not yet been investigated.

From a theoretical point of view, Mg^+ is an interesting open-shell metallic species with empty low-lying 3p orbitals, a characteristic that provides a good tool for comparison with other closed- or open-shell monocations.[13] The interest in the gaseous chemistry of Mg^+ is derived in part from its role in ionospheric processes.[14] Some data concerning the relative and absolute gas-phase binding energies of Mg^+ to different organic compounds have been published by Freiser et al.[15] Several other small complexes have been theoretically investigated and recently compilated.[1]

As part of our investigations[13] of bond activation of organic molecules by Mg^+, we report here an experimental mass spectrometry study of the decomposition of $MgCp^+$, using mass-analyzed ion kinetic energy (MIKE) and collision-activated dissociation (CAD) spectra. To explain the behavior of this system, theoretical high-level ab initio calculations have been performed for the complexes experimentally detected. Several mechanisms are also proposed to explain both the spontaneous and the activated dissociations.

In this respect, we have considered those structures resulting from the attachment to or the C−C and C−H insertions of Mg^+ into the cyclopentadienyl radical, as well as the structure resulting from the dissociation of $MgCp^+$, which yields a bisligated Mg^+ species such as $[C_2H_2-Mg-C_3H_3]^+$. On the basis of experimental findings, we have also investigated three others systems, namely, $C_5H_4Mg^{\bullet+}$, $C_3H_3Mg^+$, and $C_3H_2Mg^{\bullet+}$.

In this work after an initial statement on the experimental and theoretical methods, we will describe the MIKE and CAD spectra and then rationalize the most outstanding features, using a theoretical approach performed at a high level of theory using the ab initio G2(MP2) framework.

Experimental Section

The mass spectrometric experiments were recorded on a ZAB HSQ mass spectrometer.[16] The ions $MgC_5H_5^+$ were produced

S1089-5639(98)01562-X CCC: $15.00 © 1998 American Chemical Society
Published on Web 06/20/1998

from magnesocene by electron impact (EI) at 70 eV. Metastable and collision-induced dissociations occurring in the second field-free region (2nd FFR) between the magnetic and the electric analyzers were monitored by scanning the latter one.

The metastable ion reactions were studied by mass-analyzed ionic kinetic energy spectrometry (MIKES)[17] techniques. Collision-activated dissociations[18] (CAD) were performed by admitting argon as a target gas into the second drift region collision cell to reduce the parent ion signal to 70%.

Commercially available magnesocene ($Mg(Cp)_2$) was purchased from Aldrich and was used without further purification.

Computational Details

The geometries of the relevant systems under study were fully optimized at the MP2/6-31G** level. We also evaluated the harmonic vibrational frequencies at this level by using analytical second-derivative techniques. These harmonic frequencies were used to characterize the stationary points of the potential energy surfaces as either minima or transition states and to estimate the corresponding zero-point energies.

To have as reliable energetics as possible, the total energy of some of the relevant minima detected was evaluated at the G2(MP2) level proposed by Curtiss et al.[19] using the optimized geometry and the zero-point corrections (ZPE) at the level already mentioned. In the framework of this theory, the basis-set extension energy corrections were obtained at the second-order Møller−Plesset (MP2) level. The total energy is

$$E[\mathrm{G2(MP2)}] = E[\mathrm{QCISD(T)/6\text{-}311G(d,p)}] + \Delta_{\mathrm{MP2}} + \Delta E(\mathrm{HLC}) + E(\mathrm{ZPE})$$

where

$$\Delta_{\mathrm{MP2}} = E[\mathrm{MP2/6\text{-}311{+}G(3df,2p)}] - E[\mathrm{MP2/6\text{-}311G(d,p)}]$$

and

$$\Delta E(\mathrm{HLC}) = -0.19n_\alpha - 4.81n_\beta$$

Here, n_α and n_β are the number of α and β electrons, respectively, with $n_\alpha > n_\beta$.

The ZPE value obtained in the MP2/6-31G** calculation is scaled[20] by the empirical factor 0.93. It has been shown[19] that, in general, the average absolute deviation for G2(MP2) theory is 1.58 kcal/mol with respect to the experiment in some thermodynamical data.

The calculations were performed using the Gaussian94[21] series of programs. For the calculations concerning neutral cyclopentadienyl, as will be explained later, multiconfigurational calculations at the CASSCF[22] level were performed using the MOLPRO-96[23] package program.

To have a deeper knowledge of the nature of the possible Mg-containing bonds created, we have performed a topological analysis of the electronic charge density, ρ, and its Laplacian, $\nabla^2\rho$, using the atoms in molecules (AIM) theory of Bader and co-workers.[24] As has been shown, $\nabla^2\rho$ identifies regions of space where the electronic charge is locally depleted, and in this case, $\nabla^2\rho$ is positive or built up whereas the $\nabla^2\rho$ is negative. The former situation is typically associated with interactions between closed systems (ionic bonds, hydrogen bonds, or van der Waals interactions), while the latter characterizes covalent bonds, where the electronic charge is concentrated between the nuclei. There are, however, significant exceptions to this general rule, mainly when highly electronegative atoms are involved in the bonding. Hence, we have also evaluated the energy density,[25] $H(\mathbf{r})$, which does not show these exceptional features; in general, negative values of $H(\mathbf{r})$ are associated with a stabilizing charge concentration within the bonding region. We have also located the relevant bond critical points (bcp), i.e., points where the electronic charge density is minimum along the bond and maximum in the other two directions, because the values of the density, its Laplacian, and the energy density at these points offer quantitative information on the strength and nature of bonding. To take explicitly into account electronic correlation effects, this topological analysis was carried out over the MP2/6-31G** optimized geometries. The AIM analysis was performed using the AIMPAC series of programs.[26]

NBO analysis of Weinhold et al.[27] has also been performed to obtain the natural total charges for the different atoms of each system, as well as a description of the bonding, in terms of the natural atomic orbitals (or hybrids) centered on atoms of particular interest.

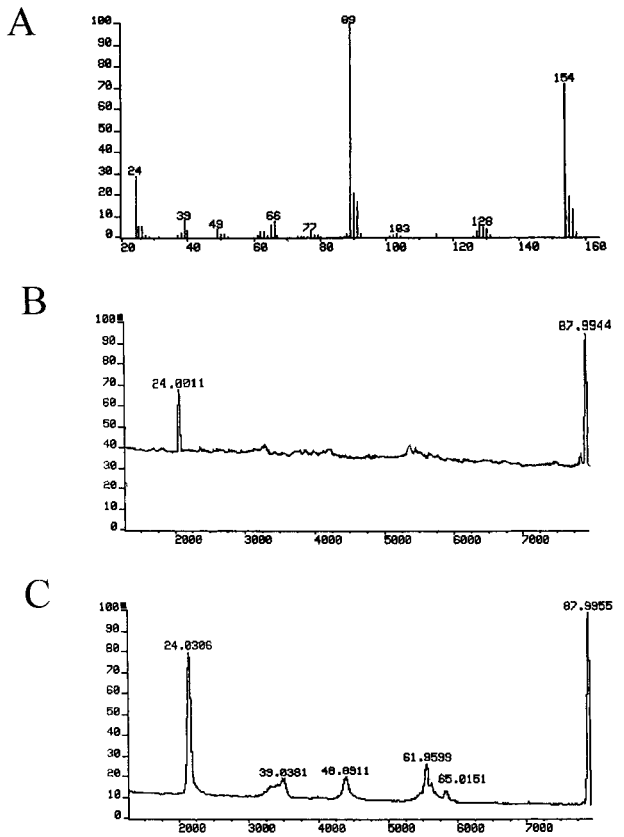

Figure 1. (A) Electronic impact (EI) spectrum of magnesocene. (B) MIKE spectrum of the $CpMg^+$ adduct at *m*/*z* 89. (C) MIKE−CAD spectrum of the $CpMg^+$ adduct at *m*/*z* 89.

Results and Discussion

Experimental Reactivity. By electronic impact, magnesocene produces an abundant $C_5H_5Mg^+$ ion at *m*/*z* 89, which is the base peak of the spectrum as shown in Figure 1A. The unimolecular behavior of the $C_5H_5Mg^+$ adduct was investigated and the MIKE spectrum (Figure 1B) of the *m*/*z* 89 ion displays two major peaks at *m*/*z* 88 and *m*/*z* 24, showing that $C_5H_5Mg^+$ undergoes fragmentation by the elimination of a hydrogen atom $H^\bullet$ and the direct cleavage of the $C_5H_5Mg^+$ adduct leading to the dissociative products Mg^+ ion and $C_5H_5^\bullet$ radical.

The metastable behavior of $C_5H_5M^+$ (M = Ti, Fe, and Rh) has been reported by Zagorevskii and Holmes.[28] These authors pointed out the fact that each species decomposes differently. So if the major metastable process is the loss of H_2 and C_2H_2

TABLE 1: Absolute (hartrees) and Relative (kcal/mol) Energies of the Systems under Study[a]

system	state	$\langle S^2 \rangle$	MP2/6-31G**	G2(MP2)	E_r MP2/6-31G**	E_r G2(MP2)
Ia	$^1A_1$		−392.305 149	−392.549 547	0.0	0.0
				−392.628 885[b]		
Ib	$^1A_1$		−392.189 501	−392.446 970	72.6	64.4
Ic	$^1A_1$		−392.152 390	−392.415 891	95.9	83.9
Id	$^1A_1$		−392.137 127	−392.400 716	105.4	93.4
C_5H_5	$^2B_1$			−193.146 897[b]		
	$^2A_2$			−193.146 453[b]		
Mg^+	^2S			−199.364 083		
$Mg^+ + C_5H_5$	$^2S + {}^2B_1$			−392.510 980[b]		74.0[b]
	$^2S + {}^2A_2$			−392.510 536[b]		74.3[b]
IIa	$^2A'$	0.777	−391.609 334	−391.858 787	0.0	
IIb	$^2A''$	0.981	−391.500 736		68.1	
IIc	$^2A''$	1.901	−391.458 751		94.5	
IId	$^2A''$	1.096	−391.454 803		97.0	
IIIa	$^1A_1$		−315.048 425	−315.212 975	0.0	0.0
IIIb	$^1A'$		−315.035 115	−315.203 922	8.4	5.7
IIIc	$^1A'$		−315.032 008	−315.198 166	10.3	9.3
IIId	$^1A_1$		−315.017 263	−315.183 102	19.6	18.7
IIIe	$^1A_1$		−315.007 274	−315.174 552	25.8	24.1
IIIf	$^1A'$		−315.007 815	−315.168 889	25.5	27.7
IIIg	$^1A'$		−315.006 449	−315.168 677	26.3	27.8
IVa	$^2A'$	0.750	−314.428 041	−314.580 545	0.0	0.0
IVb	$^2A'$	0.903	−314.366 683	−314.563 338	38.5	10.8
IVc	$^2A''$	0.977	−314.361 890	−314.544 752	41.5	22.5

[a] Contamination spin for doublet systems is also included. [b] Values without the ZPE correction.

for $C_5H_5Ti^+$ and $C_5H_5Rh^+$, respectively, the unimolecular reactivity of $C_5H_5Fe^+$ presents the same features of $C_5H_5Mg^+$ (i.e., elimination of $H^\bullet$ and metal−ligand dissociation).

Under collisional activation the adduct $C_5H_5Mg^+$ acquires sufficient internal energy to fragment by several pathways as displayed in the CAD spectrum (Figure 1C). As in the MIKE spectrum, the most important fragment ion corresponds to the loss of $H^\bullet$ giving the *m*/*z* 88 $C_5H_4Mg^{\bullet+}$ ion. Several other ions of *m*/*z* 65, *m*/*z* 63, *m*/*z* 62, *m*/*z* 49, *m*/*z* 39, and *m*/*z* 24 are present in this spectrum and are attributed, respectively, to $C_5H_5^+$, $C_3H_3Mg^+$, $C_3H_2Mg^{\bullet+}$, C_2HMg^+, $C_3H_3^+$, and Mg^+ ions. It is worth noting that ions formed under collision conditions can arise from simple bond cleavage, cyclopentadienyl ring opening, and/or consecutive neutral losses. Hence, the formation of $C_3H_2Mg^+$ can be explained by the loss of a hydrogen atom from the primary $C_3H_3Mg^+$ ion. In the same way, C_2HMg^+ can occur from $C_2H_2Mg^+$, which loses a hydrogen atom. These results suggest the intermediacy of species in which the metal ion Mg^+ is bisligated with an acetylene molecule and either a $C_3H_3^\bullet$ radical or a C_3H_2 moiety.

To corroborate this assumption and to elucidate the possible pathways leading to the observed products, we propose the study of the four systems $C_5H_5Mg^+$, $C_5H_4Mg^{\bullet+}$, $C_3H_3Mg^+$, and $C_3H_2Mg^{\bullet+}$. We will focus our attention on the structures, energetics, and bonding characteristics of different complexes and will examine the role of the open-shell ground-state $^2A_1$ of the Mg^+ ion on the $H^\bullet$ radical loss.

Theoretical Results. The previous theoretical studies[1] show the great difference between the Mg^+ π-ligand (L = C_2H_2 or C_2H_4) and the Mg^+ σ-ligand (L = oxygen- and nitrogen-containing compounds) bond energies. In the former π-complexes it is well established that the bonding is mainly electrostatic, although the open-shell 3s orbital of Mg^+ presents some 3p character, which polarizes away from the ligands to reduce the repulsion Mg^+−L, which consequently enhances the binding.

In the complexes investigated here the ligands are either open-shell ($C_5H_5^\bullet$ and $C_3H_3^\bullet$ radicals) or closed-shell (C_5H_4 and C_3H_2 carbenes) systems. To our knowledge, no study has been devoted to the reactivity of the ground state of Mg^+ with such compounds, which are also of interest in the field of ionospheric reactivity.

The total and relative energies of the different isomers for each system are listed in Table 1. In the following discussion the relative energies are always referred to the most stable ion of each series.

$C_5H_5Mg^+$ Ions: Ia−Id. Keeping in mind the observed reactivity, four $C_5H_5Mg^+$ structures (**Ia**−**Id**) have been considered (see Figure 2). The most stable species **Ia** corresponding to the association of Mg^+ with the cyclic radical c-$(C_5H_5)^\bullet$ can be described as a η^5-bonded structure having a C_{5v} symmetry where the metal is located above the center of the C_5H_5 ring. The bonding in the $^1A_1$ ground state of $C_5H_5Mg^+$ can result from several contributions as discussed below on the basis of topological and NBO analysis.

The topological analysis of this species shows that the interaction is rather typical of an ionic bond. This is mirrored in the characteristics of the Mg−Cp bond, which presents a low electron density (see Table 2) for the five equivalent bond critical points, as well as positive values for the Laplacian ($\nabla^2\rho$) and energy density ($H(\mathbf{r})$). Surprisingly, the NBO analysis predicts a natural charge of 1.8 for Mg. This interesting feature implies that the structure **Ia** could be considered as a Mg^{2+} interaction with the $C_5H_5^-$ anion. The stability of this structure may be enhanced by the fact that such a redistribution of the charge allows the system $C_5H_5^-$ to follow Huckel's rules of aromaticity. The bonds in the **Ia** system also present a covalent character as shown in the canonical MO's involved in the metal cation bonding. The interaction of the $3sp_z$ hybrid and $3p_x$, $3p_y$ pure orbitals of Mg with the 2p orbital of the five carbons leads to three doubly occupied MO's, namely, ψ_{19}, ψ_{22}, and ψ_{23} (see Figure 3). The first one is a bonding interaction of a hybrid $3sp_z$ of Mg with the π-cloud of the C_5H_5 moiety. The other two (which are the HOMO's) are made by the interaction of the "pure" $3p_x$ and $3p_y$ empty orbitals of Mg with the adequate linear combination of the five p orbitals of carbon atoms in order to maximize the bonding overlap. These three molecular

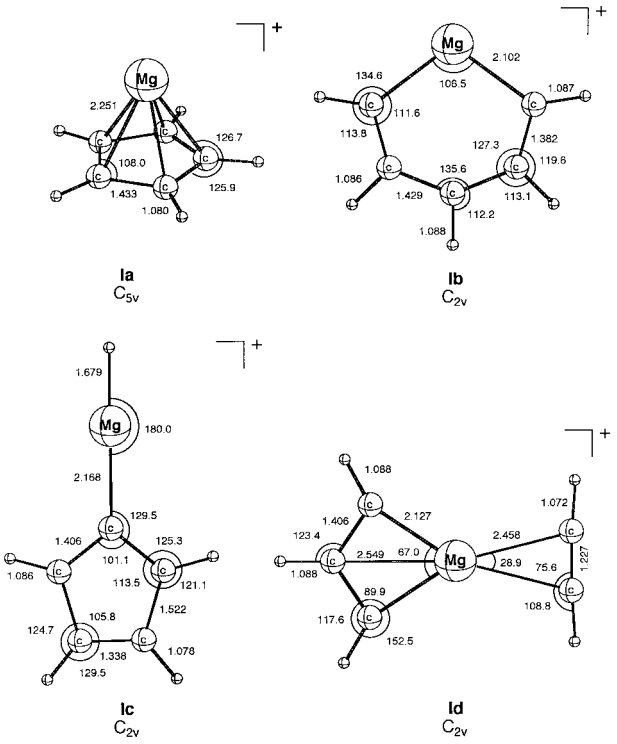

Figure 2. MP2/6-31G(d,p) optimized geometries for the minima of the $[C_5, H_5, Mg]^+$ potential energy surface. Bond distances are in angstroms and angles in degrees.

TABLE 2: Mg^+ Natural Charge, Charge Densities (ρ), Laplacian of the Charge Densities ($\nabla^2\rho$), and Energy Densities (H(r)) Evaluated at the Corresponding Bond Critical Point[a]

	bond	ρ	$\nabla^2\rho$	H(r)	Mg^+ charge
Ia	Mg−C	0.034	0.185	+0.003	1.80
Ib	Mg−C	0.051	0.278	+0.003	1.64
Ic	Mg−C	0.043	0.231	+0.003	−1.47
	Mg−H	0.054	0.242	−0.003	−0.60[b]
Id	Mg−C	0.046	0.252	+0.003	1.61
	Mg−π	0.023	0.101	+0.003	
IIa	Mg−CH	0.033	0.181	+0.003	1.80
	Mg−C	0.034	0.186	+0.003	
IIIa	Mg−C	0.064	0.389	+0.001	1.75
IIIe	Mg−C	0.047	0.257	+0.003	1.63
IIIf	Mg−C	0.040	0.141	−0.002	0.98
IVa	Mg−C	0.034	0.172	+0.003	0.95
IVb	Mg−C	0.062	0.378	+0.002	1.71

[a] All values in au. [b] This value corresponds to the natural charge of Mg attached hydrogen.

orbitals can hold the six electrons, according to Huckel's rules of aromaticity.

To estimate the $Mg^+\cdots$c-$(C_5H_5)^\bullet$ binding energy, we need the G2(MP2) energy of the $C_5H_5^\bullet$ radical. All the attempts to optimize this radical at the MP2/6-31G** led to a structure whose force calculations presented one imaginary frequency. This transition state corresponds to the opening of the ring, yielding C_2H_2 and $C_3H_3^\bullet$ fragments. This result is in accordance with the fact that the MP2 level is not appropriate for describing this system, which is well-known to be a Jahn−Teller distorted structure as described by several authors.[29] So we have considered it to be interesting to perform additional calculations using multiconfiguration SCF (MCSCF) wave functions. The main problem in this system is the degeneracy of the valence orbitals, which leads to a Jahn−Teller split of a few kcal/mol between the $^2A_2$ and $^2B_1$ states belonging to the C_{2v} point group. A starting ROHF wave function was optimized with the configuration $(9a_1)^2(6b_2)^2(1b_1)^2(2b_1)^1(1a_2)^2$ using the correlation-consistent double-ζ Dunning functions[30] in order to generate the guess wave function for the multiconfigurational calculation of the $^2B_1$ state, which will be considered as the ground state. The orbital space for the CASSCF functions was chosen by including the five valence electrons of C_5H_5 and a total number of four b_1- and two a_2-symmetry-type orbitals as the active orbital space. The geometry of the cyclopentadienyl radical has been optimized by imposing C_{2v} symmetry and placing the molecule in the *yz* plane, the *z* being the binary symmetry axis. To check the validity of active space, we have enlarged this with one additional virtual orbital of both b_1 and a_2 symmetries. This optimized geometry is rather close to the first (see Table 3), consistent with the fact that the new orbitals added present insignificant occupation numbers in the CASSCF wave function (less than 0.003). For the $^2A_2$ state, a similar procedure was performed, starting with the $(9a_1)^2(6b_2)^2(1b_1)^2(2b_1)^2(1a_2)^1$ ROHF configuration and using the same active space as for the $^2B_1$ state. Inspection of the geometries for both states in Table 3 shows that for $^2B_1$ a great contribution of the dienic structure is expected, while for the $^2A_2$ state only the C−C perpendicular to the symmetry binary axis presents double bond character. This is in agreeement, as we can see in Table 3, with results of all the other theoretical, previous studies. The maximum deviations of our results with respect to the previous calculations are 3% for the bond distances and less than 1% for the bond angles.

Finally, we used the $^2B_1$ and $^2A_2$ optimized structures to evaluate the absolute energy at the G2(MP2) level (except for the ZPE correction). The difference between them is only 0.3 kcal/mol at this level of theory. Since this value is under precision, we cannot ensure the symmetry of the ground state, but this quasi-degeneracy allows us to estimate the $Mg^+\cdots C_5H_5^\bullet$ binding energy to be 74.0 kcal/mol. For the similar complex $C_5H_5^\bullet\cdots Fe^+$, the binding energy was calculated to be 77 ± 10 kcal/mol by Bauschlischer et al.,[31] compared with an experimental value of 88 ± 7 kcal/mol. This result corroborates the fact that the $[Mg-Cp]^+$ is highly stabilized by the particularities of its charge distribution, which allows ring aromaticity.

Among the vibrational frequencies computed for the complex $Mg-Cp^+$ (**1a**) (see Table 4), there are only two skeletal modes corresponding to the metal−ring interaction that are of interest: the Mg−ring stretch and the Mg−ring bend, predicted to be observed at 477 and 307 cm^{-1}, respectively. All the other frequencies are attributed to the ring deformations. The influence of the positive charge in $MgCp^+$ can be estimated if we compare the Mg−ring stretch frequency with the value of 330 cm^{-1} reported by Robles et al.[32] for the neutral system. This is in accordance with the fact that in the ionic species the interaction of metal with C_5H_5 is stronger.

Structure **Ia** can evolve to **Ib** and **Ic,** which results from the insertion of the metal ion Mg^+ into a C−C and C−H bond of c-$(C_5H_5)^\bullet$, respectively. The structure **Ib**, corresponding to the insertion of the metal into the ring, is about 65 kcal/mol less stable than **Ia**. This is not surprising if one takes into account that the system loses its aromatic character. As revealed by its energy density on the bcp, the C−Mg−C bonds are essentially electrostatic in nature. However, by comparison with **Ia**, a lower electron transfer from Mg has been produced. The covalent contribution arises here from two three-centered orbitals formed by the interaction of the linear contribution of the 2p orbitals, in phase with each contiguous carbon, with the 3s and $3p_x$ orbitals of Mg (see Figure 4). The contour maps of the

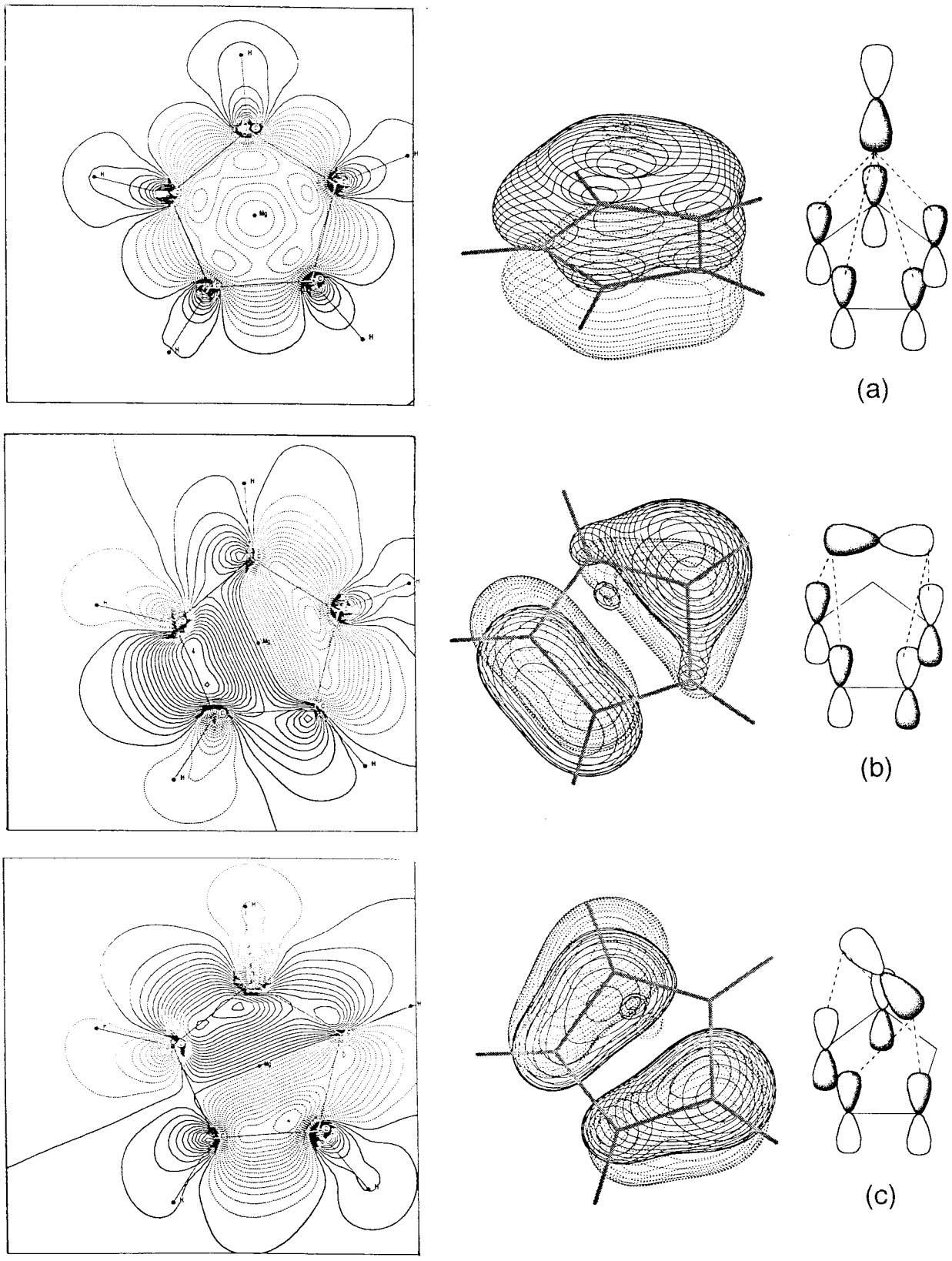

Figure 3. Doubly occupied canonical molecular orbitals for species **Ia** involved in the Mg−Cp bonding.

Laplacian of the charge density (given as Supporting Information) reveal an almost closed-shell interaction of Mg with the polarized electronic cloud of terminal carbons in the C_5H_5 moiety.

Energetically speaking, **Ic** is 83.9 kcal/mol less stable than **Ia**. In structure **Ic**, which corresponds to the insertion of Mg into a C−H bond, the positive charge is mainly localized at the Mg−H subunit, thus mirroring an interaction between the MgH^+ and the C_5H_4 moiety. Two 3sp hybrid orbitals of Mg overlap with the appropriate orbitals of carbon and hydrogen atoms. The charge of Mg is also about 1.5. It is worth noting that both in **Ib** and in **Ic** systems only two out-of-plane-type π-orbitals remain doubly occupied, avoiding aromaticity of the subsystem C_5H_4. The topological analysis points out that the

TABLE 3: Geometries of the CASSCF/DVZ Optimized Structures for $^2A_2$ and $^2B_1$ Electronic States of Cyclopentadienyl Radical[a]

	$^2B_1$					$^2A_2$		
	this work	this work[b]	ref 29a	ref 29f	ref 29e	this work	ref 29a	ref 29f
				Bond Lengths (Å)				
C1C2	1.441	1.440	1.457	1.428	1.397	1.401	1.407	1.378
C2C3	1.371	1.370	1.371	1.348	1.356	1.474	1.496	1.486
C3C4	1.485	1.484	1.509	1.514	1.442	1.359	1.396	1.338
C1H1	1.080	1.080				1.079		
C2H2	1.079	1.079				1.080		
C3H3	1.080	1.080				1.079		
				Bond Angles (deg)				
C5C1C2	108.4	108.5	108.0			107.6	108.1	
C1C2C3	107.6	107.6	108.0			108.3	108.0	
C2C3C4	108.1	108.2	108.0			107.8	107.9	
H1C1C2	125.8	125.8				126.2		
C1C2H2	125.6	125.5				126.4		
C2C3H3	126.8	126.9				125.1		

[a] C1 and H1 are the atoms containing the C_2 symmetry axis. The numbering of the other atoms is clockwise. A comparison with previous theoretical studies is also included. [b] Values corresponding to enlarged active space (see text).

TABLE 4: Harmonic Vibrational Frequencies (cm^{-1}) Assigned to $(Cp-Mg)^+$ Complex Ia

ν	symmetry	assignment
3329	a1	CH stretching
3319	e1	CH stretching
3307	e2	CH stretching
1465	e1	CC stretching
1417	e2	CC stretching
1303	a2	HCC bending in plane
1129	a1	CC stretching
1107	e2	HCC bending in plane
1040	e1	HCC bending in plane
908	e2	CH wagging
869	e2	ring deformation
850	a1	CH wagging
811	e1	CH wagging
628	e2	ring torsion
477	a1	Mg−Cp stretching
307	e1	Mg−Cp bending

Mg−C bond is an ionic interaction, whereas the Mg−H bond is covalent, as shown by the negative value of $H(\mathbf{r})$ (see Table 2).

Since one of the main features observed experimentally is the loss of acetylene under collision conditions, we have also considered the **Id** species in Figure 2. This species, which lies 93.4 kcal/mol above **Ia**, can be obtained from **Ib** by a C−C bond cleavage. In this species Mg interacts both with the $C_3H_3^\bullet$ radical and the π-cloud of acetylene. The interaction between Mg and C_2H_2 is clearly electrostatic, as demonstrated by the charge density ρ at the bcp, which is half that of Mg−C_3H_3 (see Table 2). Besides, the Laplacian of the charge density (given as Supporting Information) confirmed a closed-shell interaction of Mg with both C_3H_3 and C_2H_2 subunities (typical of ionic linkages), with the electronic cloud of both moieties being polarized toward the Mg. The charge of Mg is +1.6, showing, as observed in the case of **Ia**, an electronic transfer from the metal ion to the vinylic radical $C_3H_3^\bullet$ that thus acquires an anionic character. We have also investigated the stability of such a "sandwich" structure with a cyclopropenic radical $[c\text{-}(C_3H_3)-Mg-C_2H_2]^+$, but all attempts to optimize this geometry failed and lead to the open structure **Id**.

In summary, taking into account the estimated binding energy value between Mg^+ and $C_5H_5^\bullet$ (74.0 kcal/mol) and the fact that the relative stabilities of the other systems considered in this surface are close to or higher than this value, we may safely conclude that, from a thermodynamical point of view, the spontaneous elimination of $H^\bullet$ from the complex $C_5H_5Mg^+$ can probably arise from the most stable structure **Ia**. This is clear if one takes into account that the barrier for the C−C insertion should be higher in energy than the dissociative metal−ligand bond cleavage leading to $Mg^+ + C_5H_5^\bullet$. The C−H insertion of Mg and the opening and the cleavage of the cycle need an energetic gain. This is consistent with the experimental findings displayed in MIKE and CAD spectra (see parts B and C of Figure 1).

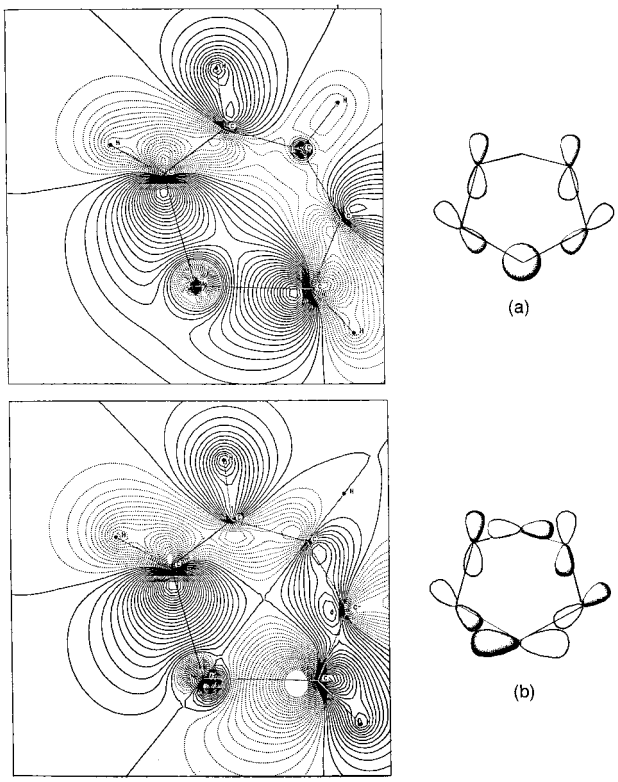

Figure 4. Doubly occupied canonical molecular orbitals for species **Ib** involved in the C−Mg−C bonding.

$C_5H_4Mg^{+\bullet}$ Ions: IIa−IId. In Figure 5 we have displayed the possible structures that can arise from the elimination of the $H^\bullet$ radical from the different precursor $C_5H_5Mg^+$ ions presented in the previous section, even if, as mentioned above, the species **Ia** would be the most probable. It is worth noting that, apart from the dissociative metal−ligand reaction, the

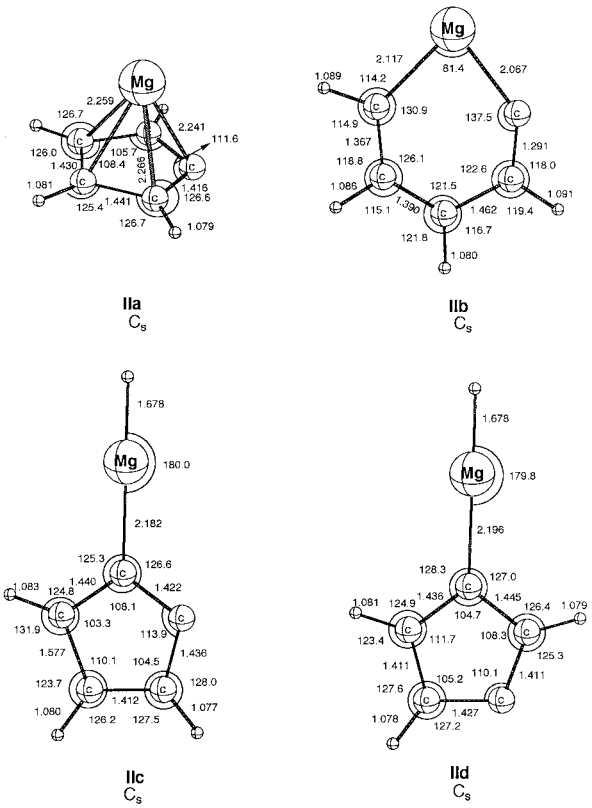

Figure 5. MP2/6-31G(d,p) optimized geometries for the minima of the $[C_5, H_4, Mg]^+$ potential energy surface. Bond distances are in angstroms and angles in degrees.

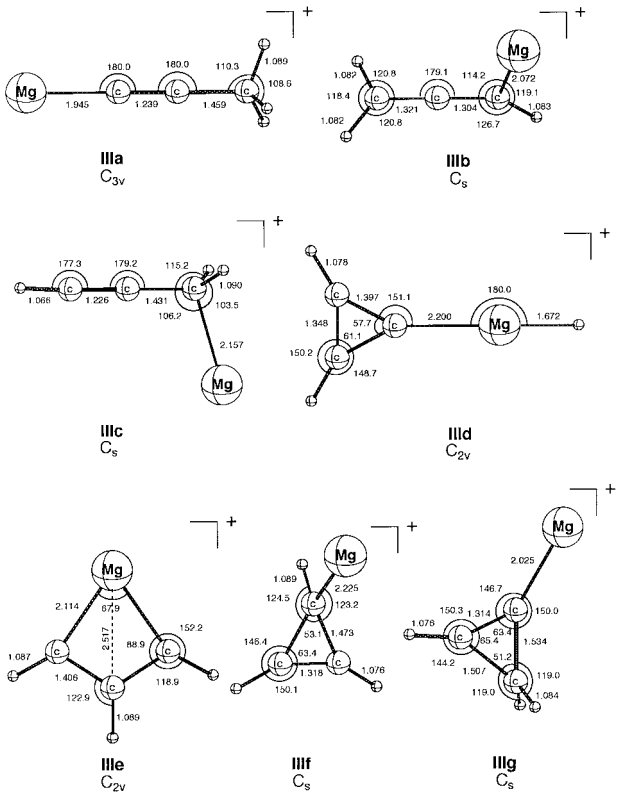

Figure 6. MP2/6-31G(d,p) optimized geometries for the minima of the $[C_3, H_3, Mg]^+$ potential energy surface. Bond distances are in angstroms and angles in degrees.

hydrogen loss is the sole efficient reaction observed in the MIKE spectrum. Among the four structures investigated the most stable (**IIa**) corresponds to the interaction of Mg ion with the aromatic moiety C_5H_4. Here too, the metal is located above the center of the C_5H_4 ring. The structure resulting from the simple abstraction of the H attached to Mg in species **Ic** has also been optimized and evolved without activation to **IIa** complex. The NBO analysis of **IIa** reveals that the charge on the Mg (1.8), the ionic bonding characteristics, and the molecular orbitals involved in the covalent component of the Mg−ring bonding are the same as for species **Ia**. The analysis of spin density shows that the unpaired electron is mainly located at dehydrogenated carbon, keeping the aromatic structure in the ring.

The G2(r) calculations show that the process to generate $MgC_5H_4^+$ starting from $MgC_5H_5^+$ requires about 120 kcal/mol, while the loss of Mg would require only 74 kcal/mol, as have been discussed. Taking into account the facts that (i) the intensity of the peak at *m*/*z* 88 is greater than that observed for the peak at *m*/*z* 240 and (ii) the difference of intensities is reduced under collision conditions (see Figure 1), we can conclude that the barriers for both dissociations play an important role and should be higher for Mg loss than for the dehydrogenation reaction.

Structures **IIb**, **IIc**, and **IId**, coming both from the elimination of H$^\bullet$ from **Ib** and from the ring positions of **Ic**, are predicted to be, respectively, 68.1, 94.5, and 97.0 kcal/mol less stable than the minimum **IIa** (at the MP2/6-31G** level). Here, it must be noted (see Table 1) that for species **IIc** and **IId** a high value of $\langle S^2 \rangle$ is predicted, revealing a nonnegligible spin contamination with higher order multiplicities.

$C_3H_3Mg^+$ Ions: IIIa−IIIg. The loss of acetylene from $C_5H_5Mg^+$ gives rise to a complex $C_3H_3Mg^+$ resulting from the interaction of a radical $C_3H_3^\bullet$ with the open-shell Mg^+ cation. We have investigated, in this part, different possible structures for the $C_3H_3Mg^+$ system (see Figure 6): those that could be derived directly from **Ia**−**Id** and those that could result from rearrangements, shown later to be more stable.

We can see in Table 1 that the global minimum for the C_3H_3-Mg^+ system corresponds to the complexation of the 1-propynyl moiety by Mg (system **IIIa** in Figure 6). A value of 1.75 for the natural charge in Mg^+ reveals without ambiguity the ionic character of the C−Mg bond that arises from the interaction of a likely Mg^{2+} with the 1-propynyl anion, where the natural charge on the carbon is −0.98. This result is not surprising if we consider that the latter is the most stable species among $C_3H_3^-$ anions.[33] The Laplacian of the charge density for this system (available as Supporting Information) shows a great interaction of Mg with C, and energy density values (see Table 2) become inferior as those observed for **I** complexes, revealing also an increase in the covalent character of Mg−C bonds. Structures **IIIb** and **IIIc** are less stable by 5.7 and 9.3 kcal/mol, respectively, and they result from the complexation of the allenide anion $C_{(3)}H_2{=}C{=}C_{(1)}H^-$ on carbon atoms $C_{(1)}$ and $C_{(3)}$ that give rise respectively to allenic (**IIIb**) and monosubstituted acetylenic (**IIIc**) structures. But even if these three structures are the most stable, under our experimental conditions they cannot originate directly from the $C_5H_5Mg^+$ cations under investigation. On the other hand, the loss of C_2H_2 from **Ic**, **Id**, and **Ib** can lead directly to less stable structures **IIId**, **IIIe**, and **IIIf**, respectively. The complexation of the cyclopropen-1 anion gives the structure **IIIg**, which is energetically degenerate with **IIIf** (see Table 1) at our level of calculation.

It is worth mentioning that **IIIe** presents almost the same structure as the subunit C_3H_3Mg of structure **Id**, showing that, as mentioned above, in **Id** the bonding of the acetylene moiety is a rather pure electrostatic interaction. The NBO and the

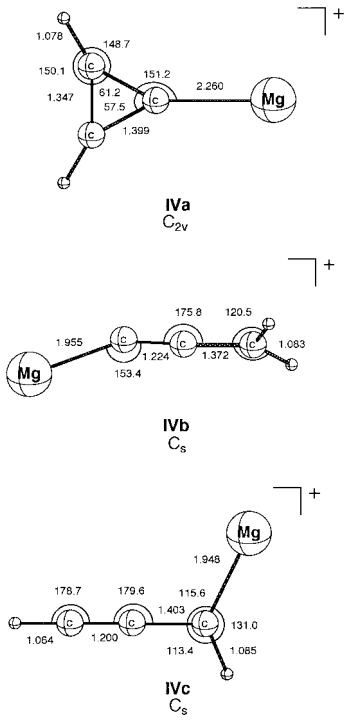

Figure 7. MP2/6-31G(d,p) optimized geometries for some of the minima of the $[C_3, H_2, Mg]^+$ potential energy surface. Bond distances are in angstroms and angles in degrees.

topological analysis of **IIIe** presents the same features concerning the charge distribution as well as the bonding characteristics (see Table 2). The case of **IIIf** is peculiar in that this structure is the sole structure where Mg has a charge close to 1 (0.98), showing that we have in fact an interaction between the open-shell $Mg^{\bullet+}$ monocation and the cyclopropenyl radical c-$(C_3H_3)^{\bullet}$. As in the case of the c-$(C_5H_5)^{\bullet}$ radical, the cyclopropenyl radical presents a Jahn−Teller effect responsible for changes in the structure and properties. This radical represents the prototype conjugated cyclic radical, which has been the subject of considerable interest.[33,34] The nonplanar structure is preferred, which is in agreement with the geometry of the Mg-cationized form **IIIf**. The cyclopropenyl anion is known to be an antiaromatic system not detected experimentally and predicted to be unbound in the gas phase.[34b] This could explain why the electronic transfer from Mg^+ to the carbon atom does not occur. The topological analysis (see Table 2) shows that in the case of **IIIf** some covalent character is mirrored in the small but negative value of the energy density $H(\mathbf{r})$.

$C_3H_2Mg^{+\bullet}$ Ions: IVa−IVc. Among the different structures investigated for $C_3H_2Mg^{\bullet+}$ ions only three have been selected and are displayed in Figure 7. All of them could be considered as the interaction of Mg^+ with different C_3H_2 carbenes and probably result from the hydrogen atom elimination from the $C_3H_3Mg^+$ structures described below. The global minimum for this series **IVa** corresponds to the cationization of the cyclopropenyl carbene, which can arise from the four cyclic species **IIId−IIIg**. It is worth noting that the linear compounds **IVb** and **IVc** are less stable than the cyclic one **IVa.**

For the complex **IVb**, the NBO analysis shows that the charge of the magnesium and those of the carbon atom Mg···C(1) are 1.71 and 0.84, respectively (see Table 2); the unpaired electron has been localized on the methylenic carbon atom $C(3)H_2$, reflecting the distonic character of the **IVb** species. On the other hand, the bonding characteristics of the global minimum **IVa** are quite different; an inspection of canonical orbitals shows that a 3s orbital of Mg interacts with a 3p orbital of the carbon atom to give a doubly occupied C−Mg bonding orbital. However, the unpaired electron is located in an orbital with antibonding character between C and Mg, which makes the bond less stable. This can be confirmed by the fact that the optimization of the corresponding neutral complex starting from the **IVa** structure leads to Mg···C cleavage.

From these theoretical results we propose in Scheme 1 different pathways that could account for the decomposition patterns of $C_5H_5Mg^+$ ions leading to fragment ions $C_5H_4Mg^{\bullet+}$, $C_3H_3Mg^+$, and $C_3H_3Mg^{\bullet+}$ here under investigation. It must be mentioned that the formation of linear $C_3H_3Mg^+$ ions (**IIIa−**

SCHEME 1: Proposed Mechanisms for Cp−Mg^+ Leading to the Reaction Products Observed Experimentally

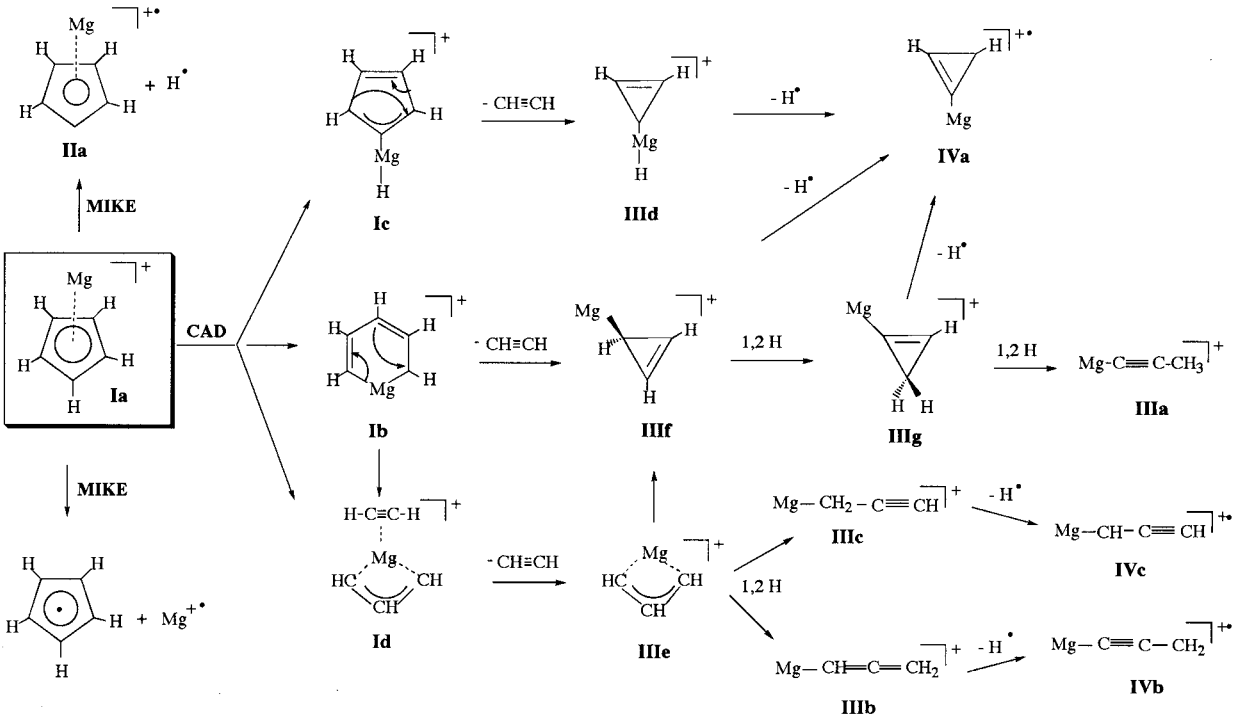

IIIc) can be envisaged as occurring from the cyclic isomers by 1,2-hydrogen shifts. These hydrogen transfers have not been calculated but they are well-known to be energy-demanding processes[13b] that can occur under collisional activation.

Conclusions

The first experimentally observed feature of magnesocene under electronic impact is the cyclopentadienyl cleavage, which generates the rather stable $MgCp^+$ complex. The structure of this system has been analyzed by using high-level ab initio methods, revealing the nature of the $Mg-Cp^+$ bonds and allowing a discussion of its covalent and ionic contributions. We can conclude that the stability of the global minimum is due to a partial charge transfer from Mg to the ring, which makes aromaticity possible. A multiconfigurational study of the Jahn−Teller split present in the cyclopentadienyl radical allowed us not only to propose geometrical parameters for both electronic states of such splitting but also to estimate a rather accurate value of 74.0 kcal/mol for the $Mg-Cp^+$ binding energy. The vibrational analysis of this system has also been performed on the other minima in the $[C_5,H_5, Mg]^+$ surfaces, since loss of hydrogen is the main feature observed experimentally in MIKE conditions. The relative energies of the different complexes involved have also been calculated at the G2(MP2) level, concluding that the observed $H^\bullet$ loss might arise mainly from the **Ia** complex, since it would lead to **IIa** complex where aromaticity and charge distribution is retained. The nature of the bonds involving Mg^+ have been studied in depth by means of NBO and topological analysis.

In addition, for the experimentally observed loss of acetylene and acetylene + $H^\bullet$ under collision conditions, we have studied the corresponding minima of surfaces $[C_3, H_3, Mg]^+$ and $[C_3, H_2, Mg]^{\bullet+}$ at the same level of theory. The most stable for $C_3H_3Mg^+$ corresponds to complexation of the 1-propynyl moiety by Mg^+ but cannot originate directly from the $C_5H_5Mg^+$ global minimum. For $[C_3, H_2, Mg]^{\bullet+}$ complexes, the global minimum corresponds to the cationization of the cyclopropenyl carbene, being only ca. 10 kcal/mol more stable than the distonic ion corresponding to the association of Mg^+ to the H_2C_3 system.

Finally, we have schematized all the theoretical results and proposed some possible pathways leading to the experimentally observed structures.

Acknowledgment. A. Luna acknowledges the European Community for a TMR grant.

Supporting Information Available: Two figures showing contour maps of the Laplacian of the charge density of species **Ia**−**Id** and contour maps of the Laplacian of the charge density of species **IIIa**, **IIIf**, and **IIIe** (2 pages). Ordering information is given on any current masthead page.

References and Notes

(1) See, for example, the following. *Organometallic Ion Chemistry*; Freiser, B. S., Ed.; Kluwer Academic Publishers: Dordrecht, 1995 and references therein.

(2) (a) Grade, H.; Cooks, R. G. *J. Am. Chem. Soc.* **1978**, *100*, 5615. (b) Bouchonnet, S.; Hoppilliard, Y.; Ohanessian, G. *J. Mass Spectrom.* **1995,** *30*, 172. (c) Rieter, A.; Adams, J.; Zhao, H. *J. Am. Chem. Soc.* **1994**, *116*, 7827. (d) Wen, D.; Yalcin, T.; Harrison, A. G. *Rapid Commun. Mass Spectrom.* **1995**, *9*, 1155. (e) Nelson, R. W.; Hutchens, T. W. *Rapid Commun. Mass Spectrom.* **1992**, *6*, 4. (f) Lei, Q. P.; Amster, I. J. *J. Am. Soc. Mass Spectrom.* **1996**, *7*, 722. (g) Cerda, B. A.; Wesdemiotis, C. *J. Am. Chem. Soc.* **1995**, *117*, 9734. (h) Gatlin, C. L.; Turecek, F.; Vaisar, T. *J. Am. Chem. Soc.* **1995**, *117*, 3637. (i) Chamot-Rooke, J.; Pennequin, F.; Morizur, J.-P.; Tortajada, J.; Rose, E.; Rose-Munch, F. *J. Mass Spectrom.* **1996**, *31*, 199. (j) Chamot-Rooke, J.; Tortajada, J.; Morizur, J.-P. *Eur. Mass Spectrom.*, **1995**, *1*, 471.

(3) Pierloot, K.; Persson, B. J.; Roos, B. O. *J. Phys. Chem.* **1995**, *99*, 3465.

(4) Wilkinson, G.; Cotton, F. A. *Chem. Ind. (London)* **1954**, 207.

(5) (a) Lippincott, E. R.; Xavier, J.; Steele, D. *J. Am. Chem. Soc.* **1961**, *83*, 2262. (b) Aleksanyan, V. T.; Garbuzova, I. A.; Gavrilenko, V. V.; Zakharkin, L. I. *J. Organomet. Chem.* **1977**, *129*, 139.

(6) (a) Faegri, K., Jr.; Almlöf, J.; Luthi, H. P. *J. Organomet. Chem.* **1983**, *249*, 303. (b) Blom, R.; Faegri, K., Jr.; Valden, H. V. *Organometallics* **1990**, *9*, 372. (c) Timofeeva, T. V.; Lii, J.-H.; Allinger, N. L. *J. Am. Chem. Soc.* **1995**, *117*, 7452.

(7) Ammeter, J. *J. Magn. Reson.* **1978**, *30*, 299.

(8) Kozen, A.; Nojima, S.; Tenmyo, J.; Asahi, H. *J. Appl. Phys.* **1986**, *59*, 1156.

(9) Lewis, C. R.; Dietze, W. T.; Ludowise, M. J. *J. Electron. Mater.* **1983**, *12*, 507.

(10) Robles, E. S. J.; Ellis, A. M.; Miller, T. A. *J. Phys. Chem.* **1992**, *96*, 8791.

(11) (a) Sodupe, M.; Bauschlicher, C. W. *Chem. Phys. Lett.* **1993**, *207*, 19. (b) Blom, R.; Faegri, K.; Midtgaard, T. *J. Am. Chem. Soc.* **1991**, *113*, 3230. (c) Szyperski, T.; Scherdtfeger, P. *Angew. Chem.* **1989**, *9*, 1228. (d) McKee, M. L. *J. Phys. Chem.* **1992**, *96*, 1683.

(12) Milburn, R.; Baranov, V.; Hopkinson, A. C.; Bohme, D. K. In *Proceedings of the 45th ASMS Conference on Mass Spectrometry and Allied Topics*, Palm Springs, CA, 1997.

(13) (a) Amekraz, B.; Tortajada, J.; Morizur, J.-P.; González, A. I.; Mó, O.; Yáñez, M. *J. Mol. Struct.: THEOCHEM* **1996**, *371*, 313. (b) Tortajada, J.; Leon, E.; Morizur, J.-P.; Luna, A.; Mó, O.; Yáñez, M. *J. Phys. Chem.* **1995**, *99*, 13890. (c) Tortajada, J.; Leon, E.; Luna, A.; Mó, O.; Yáñez, M. *J. Phys. Chem.* **1994**, *98*, 12919.

(14) (a) Murad, E.; Swider, W.; Benson, S. W. *Nature (London)* **1981**, *289*, 273. (b) Murad, E. *J. Chem. Phys.* **1981**, *75*, 4080.

(15) Operti, L.; Tews, E. C.; Freiser, B. S. *J. Am. Chem. Soc.* **1988**, *110*, 3847.

(16) Harrison, A. G.; Mercer, R. S.; Reiner, E. J.; Young, A. B.; Boyd, R. K.; March, R. E.; Porter, C. J. *Int. J. Mass. Spectrom. Ion Processes* **1986**, *74*, 13.

(17) Cooks, R. G.; Beynon, J. H.; Caprioli, R. M.; Lester, G. R. *Metastable Ions*; Elsevier: New York, 1973.

(18) *Collision Spectroscopy*; Cooks, R. G., Ed.; Plenum Press: New York, 1978.

(19) Curtiss, L. A.; Raghavachari, K.; Pople, J. A. *J. Chem. Phys.* **1993**, *98*, 1293.

(20) Pople, J. A.; Head-Gordon, M.; Fox, D. J.; Raghavachari, K.; Curtiss, L. A. *J. Chem. Phys.* **1989**, *90*, 5622.

(21) Frisch, M. J.; Trucks, G. W.; Schlegel, H. B.; Gill, P. M. W.; Johnson, B. J.; Robb, M. A.; Cheeseman, J. R.; Keith, T. A.; Peterson, G. A.; Montgomery, J. A.; Raghavachari, K.; Al-Laham, M. A.; Zakrzewski, V. G.; Ortiz, J. V.; Foresman, J. B.; Cioslowski, J.; Stefanow, B. B.; Nanayaklara, A.; Challacombe, M.; Peng, C. Y.; Ayala, P. Y.; Chen, W.; Wong, M. W.; Andres, J. L.; Replogle, E. S.; Gomperts, R.; Martin, R. L.; Fox, D. J.; Binkley, J. S.; Defrees, D. J.; Baker, J.; Stewart, J. P.; Head-Gordon, M.; Gonzalez, C.; Pople, J. A. *Gaussian 94*; Gaussian, Inc.: Pittsburgh, PA, 1995.

(22) (a) Werner, H.-J.; Knowles, P. J. *J. Chem. Phys.* **1985**, *82*, 5053. (b) Knowles, P. J.; Werner, H.-J. *Chem. Phys. Lett.* **1985**, *115*, 259. (c) Roos, B. *Advances in Chemical Physics: Ab Initio Methods in Quantum Chemistry II*; Lawley, K. P., Ed.; Wiley: Chichester, 1987.

(23) Werner, H.-J.; Knowles, P. J.; Almlöf, J.; Amos, R. D.; Berning, A.; Deegan, M. J. O.; Eckert, F.; Elbert, S. T.; Hampel, C.; Lindh, R.; Meyer, W.; Nicklass, A.; Peterson, K.; Pitzer, R.; Stone, A. J.; Taylor, P. R.; Mura, M. E.; Pulay, P.; Schuetz, M.; Stoll, H.; Thorsteinsson, T.; Cooper, D. L. *MOLPRO96*, Version 96.4; University of Birmingham: U.K., 1996.

(24) Bader, R. F. W. *Atoms in Molecules. A Quantum Theory*; Oxford University Press: Oxford, 1990.

(25) Koch, W.; Frenking, G.; Gauss, J.; Cremer, D.; Collins, J. R. *J. Am. Chem. Soc.* **1987**, *109*, 5917.

(26) The AIMPAC program package has been provided by Cheeseman, J. and Bader, R. F. W.

(27) Weinhold, F.; Carpenter, J. E. *The structure of small molecules and ions*; Plenum: New York, 1988; p 227.

(28) (a) Zagorevskii, D. V.; Holmes, J. L.*Org. Mass. Spectrom.* **1993**, *28*, 49. (b) Zagorevskii, D. V.; Holmes, J. L. *Organometallics*, **1992**, *11*, 3224.

(29) (a) Borden, W. T.; Davidson, E. R. *J. Am. Chem. Soc.* **1979**, *101*, 3771. (b) Olivella, S.; Sole, A.; Garcia-Raso, A. *J. Phys. Chem.* **1995**, *99*, 10549. (c) Ha, T.-K.; Gunthard, H. H. *Chem. Phys. Lett.* **1980**, *69*, 510. (d) Yu, L.; Williamson, J. M.; Miller, T. A. *Chem. Phys. Lett.* **1989**, *162*, 431. (e) Snyder, L. C. *J. Chem. Phys.* **1960**, *33*, 619. (f) Liehr, A. D. *Z. Phys. Chem.* **1956**, *9*, 338. (g) Hobey, W. D.; McLachlan, A. D. *J. Chem. Phys.*

1960, *33*, 1695. (h) Yu, L.; Cullin, D. W.; Williamson, J. M.; Miller, T. A. *J. Chem. Phys.* **1993**, *98*, 2682. (i) Yu, L.; Foster, S. C.; Williamson, J. M.; Heaven, M. C.; Miller, T. A. *J. Chem. Phys.* **1988**, *92*, 4263. (j) Meyer, R.; Grof, F.; Ha, T.; Gunthard, H. H. *Chem. Phys. Lett.* **1979**, *66*, 65.

(30) Dunning, T. H., Jr. *J. Chem. Phys.* **1989**, *90*, 1007.

(31) Sodupe, M.; Bauschlicher, C. W., Jr. *Chem. Phys. Lett.* **1993**, *207*, 19.

(32) Robles, E. S.; Ellis, A. M.; Miller, T. A. *J. Phys. Chem*. **1992**, *96*, 3247.

(33) Li, W.-K. *Croat. Chem. Acta* **1988**, *61*, 833.

(34) (a) Byum, Y.-G.; Saebo, S.; Pittman, C. U., Jr. *J. Am. Chem. Soc.* **1991**, *113*, 3689. (b) Glukhovtsev, M. N.; Laiter, S.; Pross, A. *J. Phys. Chem.* **1996**, *100*, 17801. (c) Chipman, D. M.; Miller, K. E. *J. Am. Chem. Soc.* **1984**, *106*, 6236.